Drug Design, Development and Therapy

Dovepress
open access to scientific and medical research

Open Access Full Text Article

ORIGINAL RESEARCH

Naotaifang III Protects Against Cerebral Ischemia Injury Through LPS/TLR4 Signaling Pathway in the Microbiota–Gut–Brain Axis

Huifang Nie[1], Jinwen Ge[1,2], Kailin Yang[1], Zhuli Peng[1], Haihui Wu[1], Tong Yang[1], Zhigang Mei[1]

[1]Key Laboratory of Hunan Province for Integrated Traditional Chinese and Western Medicine on Prevention and Treatment of Cardio-Cerebral Diseases, Hunan University of Chinese Medicine, Changsha, Hunan, 410208, People's Republic of China; [2]Hunan Academy of Chinese Medicine, Changsha, Hunan, 410006, People's Republic of China

Correspondence: Zhigang Mei; Jinwen Ge, Hunan University of Chinese Medicine, Changsha, Hunan, 410208, People's Republic of China, Email meizhigang@hnucm.edu.cn; 001267@hnucm.edu.cn

Background: Ischemic stroke (IS) is a leading cause of mortality worldwide. Naotaifang III is a new Chinese herbal formula to treat IS. Previous studies have shown that *Astragali Radix, Puerariae Lobatae Radix, Chuanxiong Rhizoma,* and *Rhei Radix Et Rhizoma* in Naotaifang III were able to regulate the imbalance of intestinal microbiota during cerebral ischemia injury.

Methods: Rats were randomly divided into sham operation group, normal control group, middle cerebral artery occlusion (MCAO) group, intestinal microbiota imbalance MCAO group, Naotaifang III group, and normal bacteria transplantation group, with 15 rats in each group. Then, neurological function scores and cerebral infarction volume were detected; haematoxylin and eosin staining and Golgi silver staining were used to observe morphological changes in brain tissue. Meanwhile, the lipopolysaccharide (LPS) and cerebral cortex interleukin (IL)-1β were detected by enzyme-linked immunosorbent assay (ELISA); the expressions of Toll-like receptor (TLR)-4 and nuclear factor kappa-B (NF-κB) proteins were detected by immunofluorescence and Western blot. The cecal flora was detected by 16S rDNA. The results showed that gut dysbiosis aggravated cerebral ischemic injury and significantly increased the expression of LPS, TLR4, NF-κB, and IL-1β, which could be significantly reversed by Naotaifang III or normal bacterial transplantation. Naotaifang III may exert a protective effect on neuroinflammatory injury after MCAO through the LPS/TLR4 signaling pathway in the microbe-gut-brain axis. In summary, Naotaifang III may induce anti-neuroinflammatory molecular mechanisms and signaling pathways through the microbe-gut-brain axis.

Results: The results showed that gut dysbiosis aggravated cerebral ischemic injury and significantly increased the expression of LPS, TLR4, NF-κB, and IL-1β, which could be significantly reversed by Naotaifang III or normal bacterial transplantation. Naotaifang III may exert a protective effect on neuroinflammatory injury after MCAO through the LPS/TLR4 signaling pathway in the microbe-gut-brain axis.

Conclusion: Naotaifang III may induce anti-neuroinflammatory molecular mechanisms and signaling pathways through the microbe-gut-brain axis.

Keywords: Naotaifang III, ischemic stroke, intestinal microbiota, LPS/TLR4 signaling pathway, microbiota–gut–brain axis

Introduction

Ischemic stroke (IS) is a common acute cerebrovascular accident, which accounts approximately for 79% of all strokes,[1] and has become one of the leading causes of death and disability worldwide. Recombinant tissue plasminogen activator (rt-PA) is an acute IS treatment that is limited to use within 4.5 hours of IS onset.[2] However, due to the narrow time window and potential bleeding risk, only 2–10% of IS patients worldwide benefit from thrombolysis, and only 1.2–3.8% in China.[3,4] Brain ischemic injury involves multiple mechanisms, such as inflammation, oxidative stress, calcium overload, apoptosis, and glutamate excitotoxicity. Previous studies have shown that gut microbiota may regulate cerebral ischemia injury through the microbe-gut-brain axis,[5,6] but the exact mechanism has not been fully elucidated. As the second human genome and the largest immune organ, the gut microbiota plays an important role in maintaining

Received: 17 May 2023
Accepted: 31 October 2023
Published: 1 December 2023

Graphical Abstract

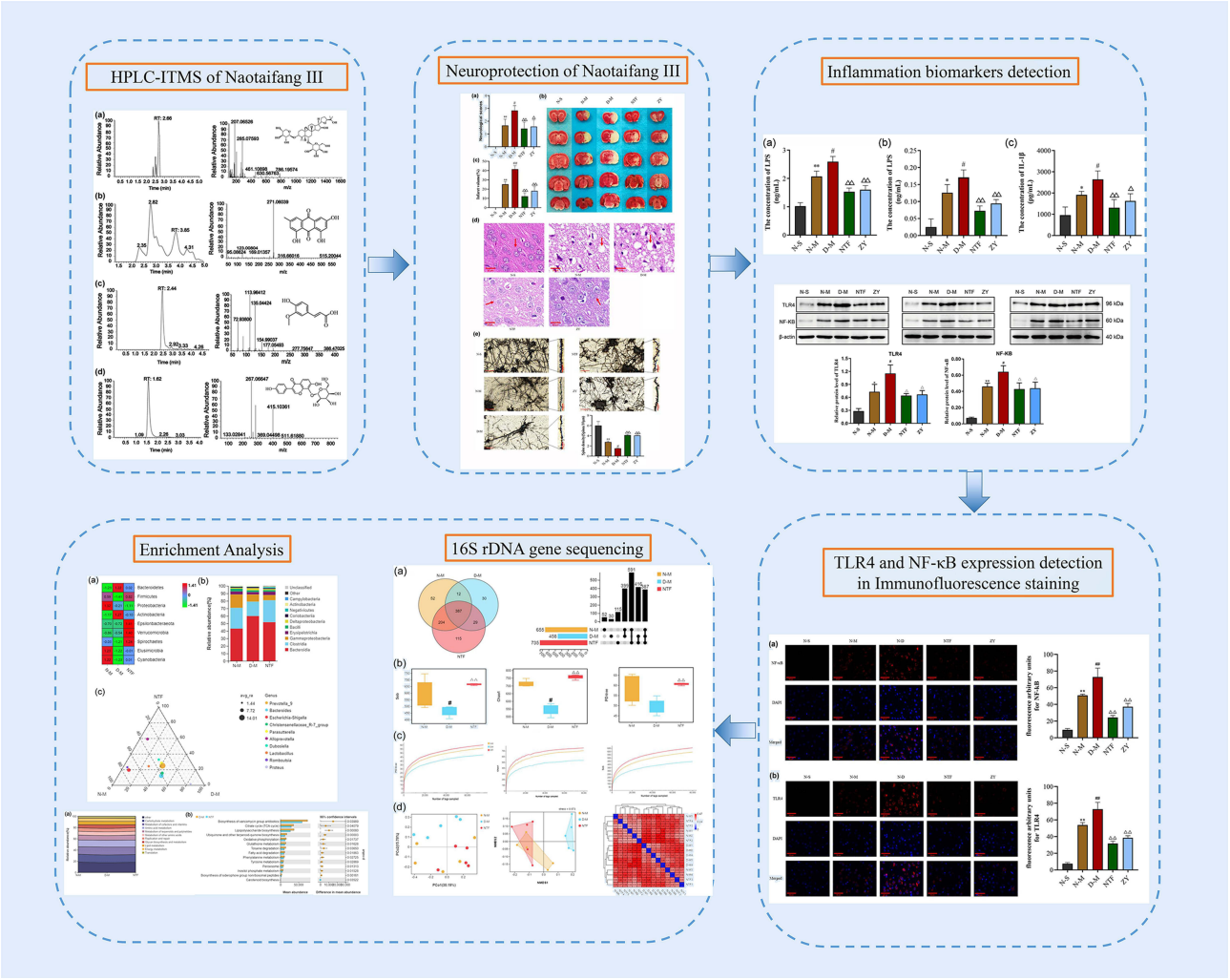

body homeostasis. Recent studies have shown that gut dysbiosis is closely related to neuroinflammatory responses.[7,8] Lipopolysaccharide (LPS) from Gram-negative bacteria is a specific ligand for TLR4, which activates the immune-inflammatory response of the body's innate immune cells.[9] After IS, the levels of LPS and D-lactic acid, which reflect gut microbiota translocation, are increased in peripheral blood.[10] Moreover, LPS is lipolytic and can cross the blood–brain barrier (BBB).[11] Therefore, dysbiosis of the gut microbiota may exacerbate neuroinflammatory damage through LPS/TLR4 signaling pathway.

Clinical studies have shown that traditional Chinese medicine (TCM) has a certain curative effect on cerebral ischemia injury.[12,13] Naotaifang is adapted from a classical prescription, Buyang huanwu Decoction, which exhibits beneficial function of nourishing *Qi* and promoting blood circulation, removing heat, and relaxing bowel according to the theory of TCM. Our previous studies have shown that Naotaifang can attenuate cerebral ischemic injury, reduce cerebral infarct size, inhibit oxidative stress and neuroinflammatory responses, and block programmed cell death processes such as apoptosis or ferroptosis.[12,14,15] However, it is unclear whether it exerts anti-neuroinflammatory effects by improving gut microbiota.

Naotaifang III is modified from Naotaifang, which is invented by Prof. Ge Jinwen and used for treating IS. It added *Puerariae Lobatae Radix, Scutellariae Radix, Rhei Radix Et Rhizoma, Taraxaci Herba, Zingibers Rhizoma, Glycyrrhiza*

Radix Et Rhizoma. Previous studies have indicated that some of the herbs and components in Naotaifang exert a function of regulating intestinal microbiota. It has been reported that the astragalus polysaccharide contained in Astragalus could balance the gut microbiota.[16] Chen et al revealed that the combination of Puerariae Lobatae Radix and Chuanxiong Rhizoma could alleviate intestinal dysbacteriosis in IS.[10] Rhubarb anthraquinone glycosides are the main active components of *Rhei Radix Et Rhizoma*, which can regulate the intestinal microbiota and exhibit the effect of inhibiting free radical damage and inflammatory response.[17] Meanwhile, our previous studies have shown that the therapy of invigorating Qi and activating blood circulation can improve the homeostasis of intestinal microbiota after cerebral ischemia.[18,19] However, the mechanism by which Naotaifang III regulates gut microbiota to protect against cerebral ischemia injury has not been fully elucidated. This study would further explore the protective mechanism of Naotaifang III against cerebral ischemia injury based on the LPS/TLR4 signaling pathway involved in the microbe-gut-brain axis, further emphasizing the gut microbiota as a potential target for TCM treatment of IS.

Materials and Methods

Preparation of the Naotaifang III

The composition of Naotaifang III is shown in Table 1, which was provided by the First Hospital of Hunan University of Chinese Medicine (Hunan, China) and authenticated by Professor Jinren Xiao, Hunan University of Chinese Medicine. All traditional Chinese medicinal materials were soaked in water for 4–6 h, decocted over moderate heat, and then purified to obtain paste powder.

LC–MS Analysis

High-performance liquid chromatography (HPLC) was utilized to qualitatively verify four representative compounds in Naotaifang III: Puerarin, Ferulic Acid, Astragaloside IV, and Emodin. After ultrasonic-assisted extraction with 80% methanol, the samples were carried out using a Atlantis T3 column (150 × 2.1 mm, 3 μm) by gradient elution using 0.1% formic acid solution and acetonitrile as the mobile phase at a flow rate of 0.4 mL/min, and the column temperature was 35°C. The gradient elution flow rate: 0.4 mL/min, the elution program was as follows: 0–1.0 min, 80%A: 20%B; 1.0–3.0 min, 35%A: 65%B; 3.0–4.0 min, 5%A: 95%B; 4.0–4.2 min, 80%A: 20%B; 4.2–5.0 min, 80%A: 20%B; Data were acquired and analyzed using Xcalibur (Thermo) software.

Animals and Treatments

One hundred eighty-nine male Sprague–Dawley (SD) rats (7–9 weeks old, 240–260 g) were purchased from Hunan SJA Laboratory Animal Co., Ltd. (Changsha, China). Rats were housed in the SPF-level barrier room at the Experimental Animal Center of Hunan University of Chinese Medicine under standard light and dark cycling conditions (12/12 h, temperature 22–25°C) and were fed sterilized feed and sterile water throughout the whole process. All animal care and

Table 1 Drug Composition of Naotaifang III

Chinese Medicine	Family	Weight (g)
Huang Qi (*Astragali Radix*)	Legume	30
Ge Gen (*Puerariae Lobatae Radix*)	Legume	24
Di Long (*Pheretima*)	Euphorbiidae	12
Chuan Xiong (*Chuanxiong Rhizoma*)	Apiaceae	12
Jiang Can (*Bombyx Batryticatus*)	Saturniidae	9
Huang Qin (*Scutellariae Radix*)	Lamiaceae	12
Da Huang (*Rhei Radix Et Rhizoma*)	Polygonaceae	15
Pu Gongyin (*Taraxaci Herba*)	Compositae	12
Gan Jiang (*Zingibers Rhizoma*)	Zingiberaceae	12
Gan Cao (*Glycyrrhiza Radix Et Rhizoma*)	Legume	3

protocols were performed in accordance with the *Guidelines for Animal Experimentation* and were approved by the Animal Ethics Committee of Hunan University of Chinese Medicine.

We establish a rat model of intestinal dysbacteriosis similar to the structure and characteristics of microorganisms of IS in our previous studies (Figure 1). According to the previous method, sixty-three male SD rats performed with Middle cerebral artery occlusion (MCAO) were used as donors to breed sixty-three rats with intestinal dysbiosis. Nextly, normal SD rats (n = 18) and SD rats with intestinal dysbiosis (n = 18) were randomly selected for MCAO (N-M and D-M groups), and three rats were, respectively, chosen for test of neurological function score and cerebral infarction volume at 6h, 12h, and 24h postoperatively.

Subsequently, thirty normal SD rats were randomized into two groups: the sham-operated (N-S) group (n = 15), the MCAO (N-M) group (n = 15); and forty-five intestinal dysbiosis SD rats were randomized into three groups: the MCAO of intestinal dysbiosis (D-M) group (n = 15), Naotaifang III (NTF) group (n = 15), normal bacteria intragastric transplantation (ZY) group (n = 15). The N-S, N-M, and D-M group were gavaged with sterile water for 3 days (two days before surgery and the day of surgery). The NTF group was gavaged with Naotaifang III for 3 days (two days before surgery and the day of surgery, 11.34g/kg/day). The ZY group was gavaged with supernatant of cecal contents of normal rat for 3 days (two days before surgery and the day of surgery, 2mL/day). The dose of Naotaifang III converted according to the ratio of human and rat body surface area was 11.34g/kg/day. Rats were gavaged once daily with a volume of 1mL/100g/day. Gavage with normal bacteria was chosen as a positive control therapy (Figure 2).

Animal Modeling Methods

After the rats were anesthetized by intraperitoneal injection of 3% pentobarbital sodium 1 mL/kg, a 2-cm longitudinal incision was made in the middle of the neck, the neck muscles were bluntly separated, and the right common carotid artery (CCA), the internal carotid artery (ICA), the external carotid artery (ECA), and the vagus nerve were exposed and separated. A 0.2 mm "V"-shaped incision was made 4–5 mm from the CCA bifurcation, and a 0.26 mm diameter monofilament nylon fishing line with knotted front was inserted into the internal carotid artery (ICA) through the right CCA incision, stopping when the black mark on the wire reached the bifurcation of the ICA and ECA and the wire met resistance. The distal end of the CCA was ligated. To prevent accidental slipping, the excess line was secured, the line outside the vessel was clipped, and the muscle and skin were sutured.[20]

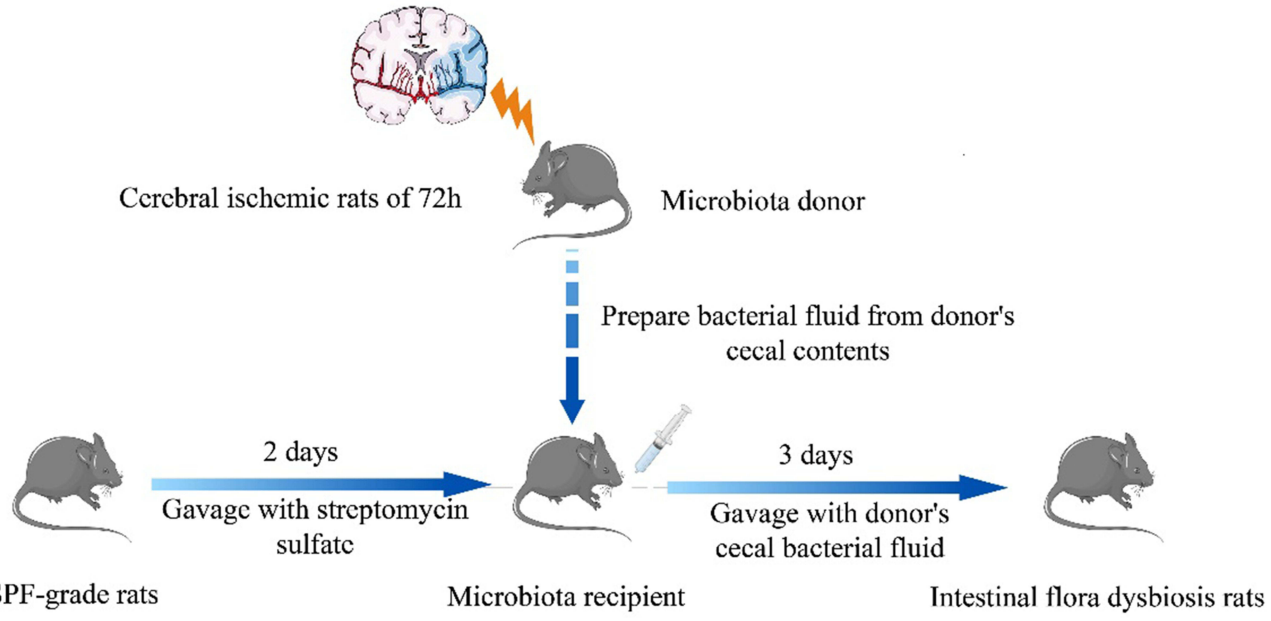

Figure 1 Establishment of the intestinal dysbacteriosis rat model.

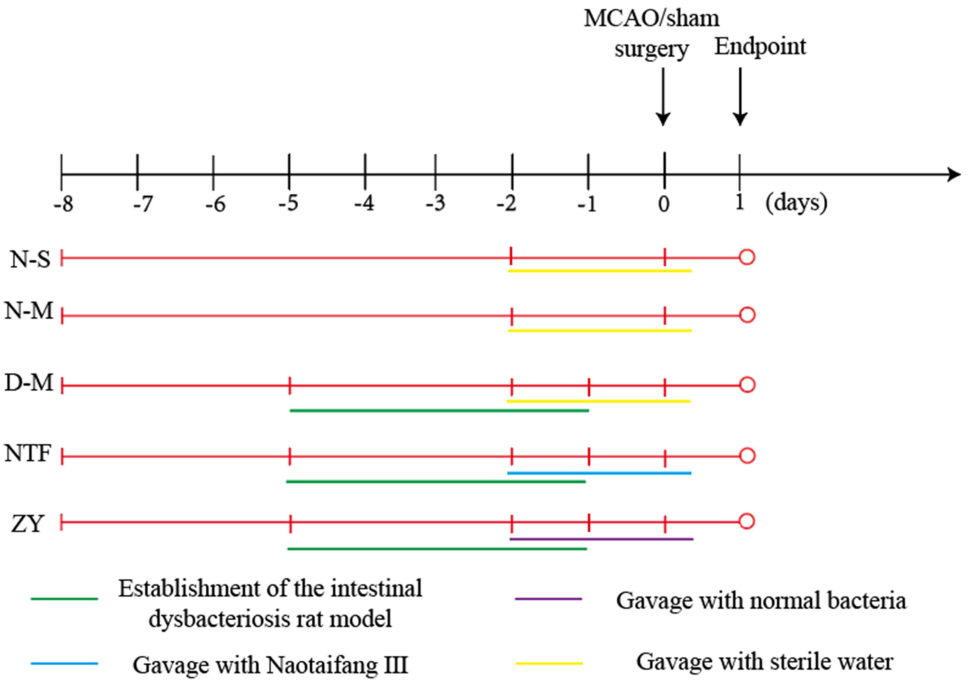

Figure 2 Treatment of each group.

Neurological Scores

Neurological scores were obtained for each group at 24 h following the MCAO, according to the method described by Longa[21] as follows. Zero score: normal, no neurological deficit; 1 score: inability to fully extend the left front paw, mild neurological deficit; 2 scores: the rat turned to the left side (temporal side) while walking, moderate neurological deficit; 3 scores: the rat inverted to the left side (temporal side) while walking, severe neurological deficit; 4 scores: inability to walk, or loss of consciousness.

2,3,5-Triphenyltetrazolium Chloride (TTC) Staining

The rats were sacrificed by cervical dislocation under anaesthesia with 2% pentobarbital sodium. The brain tissues were rapidly removed from the skull, placed on a clean glass plate, frozen at −20°C for 20 minutes, and then cut into five 2-mm-thick coronal sections by Leica cryostat CM1900 (Leica, Germany). All sections were completely stained in 2% TTC (Sigma, America) at 37°C for 30 minutes in the dark and turned over every 10 minutes. They were then fixed in 4% paraformaldehyde solution for 24 hours. Brain infarct volumes were analysed with Image-Pro Plus 6.0.

Haematoxylin and Eosin (HE) Staining

Brains were removed from 3 rats in each group and stained with HE. The whole brain was immersed in 4% paraformaldehyde for 3 days and then embedded in paraffin. Brain tissues from different groups with the same lesion were sliced into 4-μm-thick sections, which were placed in xylene I for 20 min, xylene II for 20 min, anhydrous ethanol I for 5 min, anhydrous ethanol II for 5 min, 75% alcohol for 5 min, and rinsed with tap water. The sections were immersed in haematoxylin stain for 3–5 min and then sequentially washed with tap water, differentiation solution, tap water, bluing solution, and running water. Next, the sections were sequentially immersed in 85% and 95% gradient alcohols and then in an eosin staining solution for 5 minutes. Finally, the sections were sealed with neutral glue after dehydration. The histological changes in brain tissue were observed by microscopy.

Golgi-Cox Staining

Brains were disconnected from 3 rats in each group and stained with Golgi-Cox. The solution A: solution B ratio was 1:1 for tissue fixation, where the tissue-to-fixative ratio was 1:5. The brains were stored in the dark for 1 day and then

transferred into a fresh Golgi-Cox solution for 14 days. Then, the brains were immersed in solution C for 3–7 days, and the solution was changed every 24 h. The ratio of solution D to solution E to distilled water was 1:1:2. The brains were sectioned, dried at room temperature for 3 days, washed with distilled water, and restained with solutions D and E. Finally, all sections were subjected to gradient ethanol dehydration, xylene transparency, coverslipping, and neutral resin sealing.

Immunofluorescence Staining

Immunofluorescence (IF) was performed to detect the TRL4 and NF-κB expression. First, the paraffin sections were dewaxed in water. The embedded sliced tissue sections were sequentially put into xylene I and xylene II for 15 mins and then anhydrous ethanol I, anhydrous ethanol II, 85% alcohol, 75% alcohol, and distilled water for 5 min each. Second, for antigen repair, the tissue sections were immersed in a cassette of citric acid antigen repair buffer (pH 6.0) in a microwave oven. Care was taken during this procedure to prevent excessive evaporation of the buffer. After natural cooling, the slides were immersed in PBS (pH 7.4) and washed 3 times for 5 min each with shaking on a decolorizing shaker. Third, the slides were removed from PBS, the blocking solution was shaken off, PBS containing TLR4 (CST, America) diluted 1:100 and NF-κB (CST, America) diluted 1:100, separately, was added dropwise onto the sections, and the sections were incubated flat in a wet box at 4°C overnight. Next, the slides were removed from the wet box, soaked in PBS (pH 7.4), and washed 3 times with shaking on a decolorizing shaker for 5 min each time. The slides were then removed, the PBS was gently shaken off the slides, the corresponding HRP-conjugated secondary antibody was added in a circle to cover all the tissue, and the slides were incubated for 50 min at room temperature away from light. The slides were soaked in PBS (pH 7.4), washed 3 times with shaking on a decolorization shaker for 5 min each, and then incubated with 488-TSA for 30 min. Then, we repeated the above procedure from antigen repair to adding the primary antibody and secondary antibody. All sections were viewed under a fluorescence microscope for observation and image acquisition.

IL-1β and LPS ELISAs

The levels of IL-1β and LPS cytokines in the cerebral cortex and LPS in plasma were quantified using specific ELISA kits according to the manufacturer's instructions (IL-1β, sigma, America; LPS, Cusabio, Wuhan, China).

Western Blot Analysis

Western blotting was used to detect the levels of TLR4 and NF-κB protein in rat brain cortex areas. Equal amounts of proteins were added to 50 μL of lysis buffer. Samples were centrifuged at 12,000 r/min for 10 min at 4°C. SDS–PAGE was performed with a 10% separation gel and 5% stacking gel, and the proteins were transferred to a 0.45 μm polyvinylidene fluoride membrane. The membranes were blocked in TBS-T containing 5% nonfat milk for 1 hour. The membranes were incubated with primary antibody [NF-Kb (Cat. No.: AF5006, Affinity Inc.) 1:1000; TLR4 (Cat. No.: AF7017, Affinity Inc.) 1:1000] at 4°C overnight. After washing, the membrane was incubated with the secondary antibody [Anti-Rabbit IgG (H+L) Antibody (Cat. No.: 074-1506, KPL Inc.) 1:5000] for 1 hour at room temperature. Proteins were visualized by electrochemiluminescence (ECL). The cumulative optical density of relative protein expression was assessed using ImageJ software (V1.8.0, NIH).

16Sr DNA Gene Sequencing

Five rats in each group of N-M, D-M, and NTF were randomly selected, and 16S rDNA sequencing was used to assess the intestinal microbiota in the caecum after 24h of cerebral ischemia. Genomic DNA was extracted from the samples using a stool DNA extraction kit, the purity of the nucleic acids was assessed with a NanoDrop microspectrophotometer, and the integrity of the nucleic acid samples was examined by agarose gel electrophoresis. The V3–V4 region of the 16S rDNA was amplified using 341F (5′-CCTACGGGNGGCWGCAG-3′) and 806R (5′-GGACTACHVGGGTATCTAAT-3′) primers. The purified amplicons were sequenced on the Illumina HiSeq platform (HiSeq 2500; Illumina, Inc., San Diego, CA, USA) to generate paired-end reads (2 × 250 bp). After sequencing the raw reads, the low-quality reads were first filtered and then assembled, the double-ended reads were spliced into tags, and then the tags were filtered. The resulting data were called clean tags. Next, we performed clustering based on clean tags, removed the chimeric tags detected in the

clustering comparison process, and finally obtained the data as effective tags. After operational taxonomic units (OTUs) were obtained, OTU abundance statistics were performed. According to the analysis process, species annotation, α-diversity analysis, β-diversity analysis, and community function prediction were performed sequentially. If valid subgroups existed, group differences were compared, and statistical tests were performed.

Statistical Analysis

All data were analysed using SPSS 25.0 statistical software. Quantitative data are expressed as the mean ± standard deviation (SD). The significant differences between the groups were examined by one-way analysis of variance (ANOVA) with the least significant difference test. $P<0.05$ was considered to indicate statistical significance.

Results

Analysis of Naotaifang III Ingredients

As shown in Figure 3, four active ingredients in Naotaifang III had been performed by HPLC-ITMS, respectively. The main compounds were quantified: Astragaloside IV 9.130 ng/mg, Emodin 1863.0 ng/mg, Ferulic Acid 410.6 ng/mg and Puerarin 71.7ng/mg. Analytes were quantified in multiple reaction monitoring (MRM) mode targeting the precursor ion (MS 1) to a specific fragment, which is the product ion (MS 2). The prominent ions mass spectra of the fragment ions of the four active components were as follows: Astragaloside IV 207.077m/z, Emodin 271.06m/z, Ferulic Acid 113.96m/z and Puerarin 267.07m/z. According to the optimized detection conditions, the standard solutions of 4 compounds were sampled and determined in the order of concentration from low to high, with the concentration of the substance to be tested as the Abscissa, the ratio of the peak area of the substance to be tested to the peak area of the corresponding isotope internal standard (peak area/peak area of the internal standard) as the ordinate, the standard curve, linear range, regression equation, and correlation coefficient were obtained. The results showed that the linear correlation coefficient R^2 was more than 0.999 in a wide concentration range, and the linear relationship was good.

Effects of Intestinal Microbiota Disorder on Neurological Function Score and Cerebral Infarction Volume at Different Time After Cerebral Ischemia

As shown in Figure 4a, with increasing cerebral ischemia time, the degree of neurological impairment in both groups increased progressively. The neurological function scores of the D-M group were higher at 6 h, 12 h, and 24 h than the N-M group, and the difference between the two groups was greatest at 24 h. However, the difference of neurological function scores between the two groups at the same time point was not significantly different, which might be related to the small sample of experimental animals ($n = 18$, $P > 0.05$). Moreover, the TTC staining analysis indicated that both the N-M and D-M groups had significant right-sided cerebral infarction after cerebral ischemia that increased gradually with time at 6 h, 12 h, and 24 h (Figure 4b). Compared with the N-M group, the infarct volume in the D-M group increased significantly at 12 h and 24 h, and the most significant increase was at 24 h ($n = 18$, $P < 0.01$). These results suggest that gut dysbiosis may exacerbate cerebral ischemic injury.

Effects of Naotaifang III on the Cerebral Injury

Neurological function of rats was assessed with NSS 24 h after infarction (Figure 5a). There was no neurological impairment in the N-S group. Compared with the N-S group, the neurological function scores of the N-M group were significantly increased ($n = 15$, $P < 0.05$). Compared with the N-M group, the neurological function score of the D-M group was significantly increased ($n = 15$, $P < 0.05$). However, the NTF and ZY groups had significantly lower neurological scores than the D-M groups ($n = 15$, $P < 0.01$, $P < 0.05$). The volume of cerebral infarction was observed by TTC staining. As shown in Figure 5b, no infarction was observed in the N-S group. Compared with the N-M group, the cerebral infarct volume in the D-M group was significantly increased ($n = 3$, $P < 0.01$). The volume of cerebral infarction in the NTF group and ZY group was significantly smaller than that in the D-M group ($n = 3$, $P < 0.01$). HE staining showed that the neurons in the cortical area of the the N-S group were round or oval with regular arrangement, complete nuclei, and clear nucleoli. In the N-M group, cortical edema, interstitial relaxation, irregular arrangement of neuronal

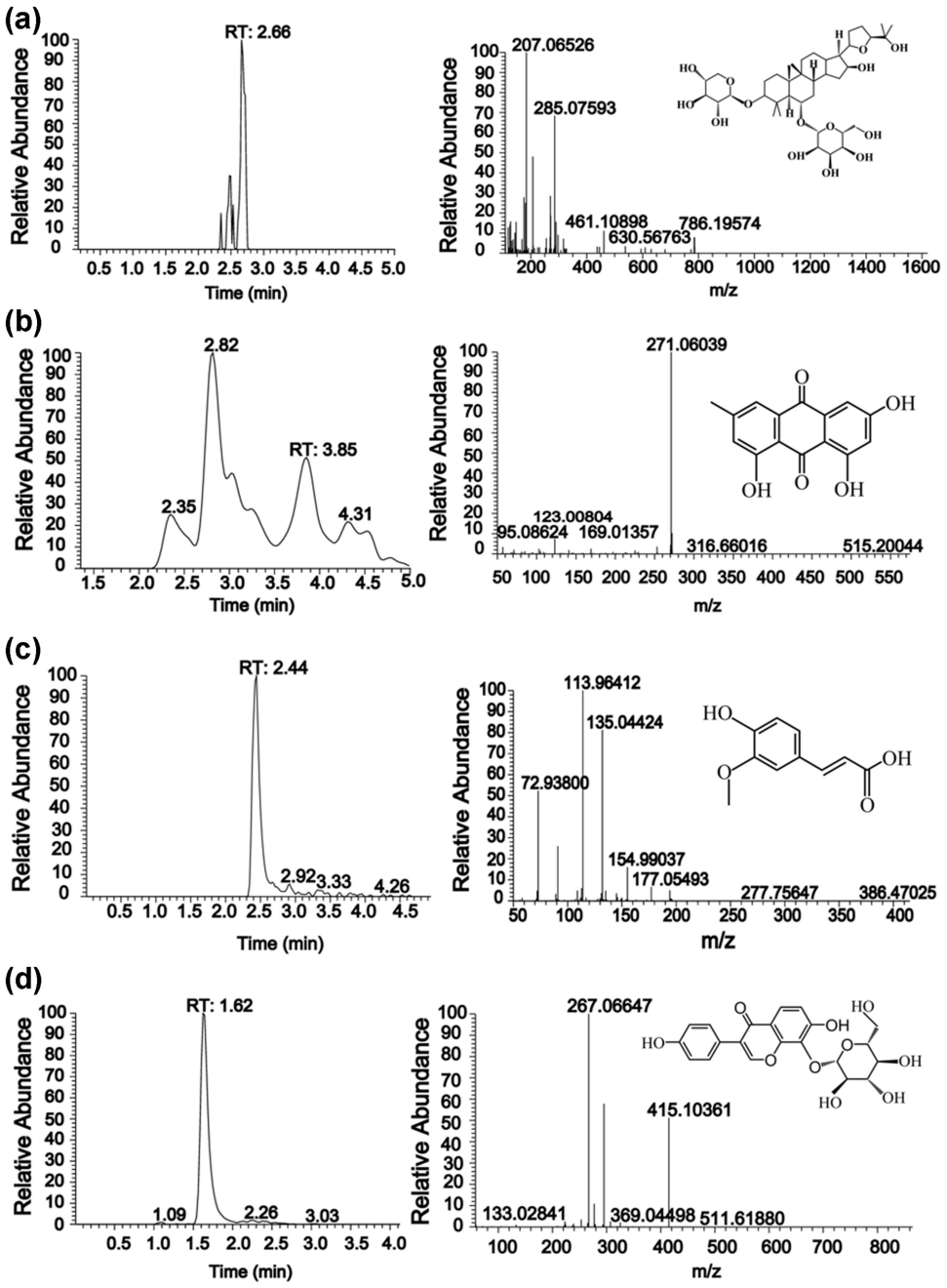

Figure 3 Quality control of Naotaifang III.
Notes: (**a**) Astragaloside_IV; (**b**) Emodin; (**c**) Ferulic_acid; (**d**) Puerarin.

cells, shrinkage of cell bodies, nuclear changes, and a large number of lymphocytes infiltration were more obvious in the D-M group. However, tissue edema and cell swelling were relatively reduced in the NTF and ZY groups, and neurofibrils were well aligned compared with the D-M group (Figure 5c). Finally, Golgi staining was used to observe the density of dendritic spines in the ischemic cortex of rats. As shown in Figure 5d, the density of dendritic spines in the N-M group was significantly reduced compared with the N-S group, and the density of dendritic spines in the D-M group was significantly reduced compared with the N-M group ($n = 3$, $P < 0.05$). However, in the NTF and ZY groups, the neuronal structure was improved, with a trend of increased dendritic spines compared to the D-M group ($n = 3$, $P < 0.01$). These results suggest that Naotaifang III can improve neurological function and cerebral ischemia injury.

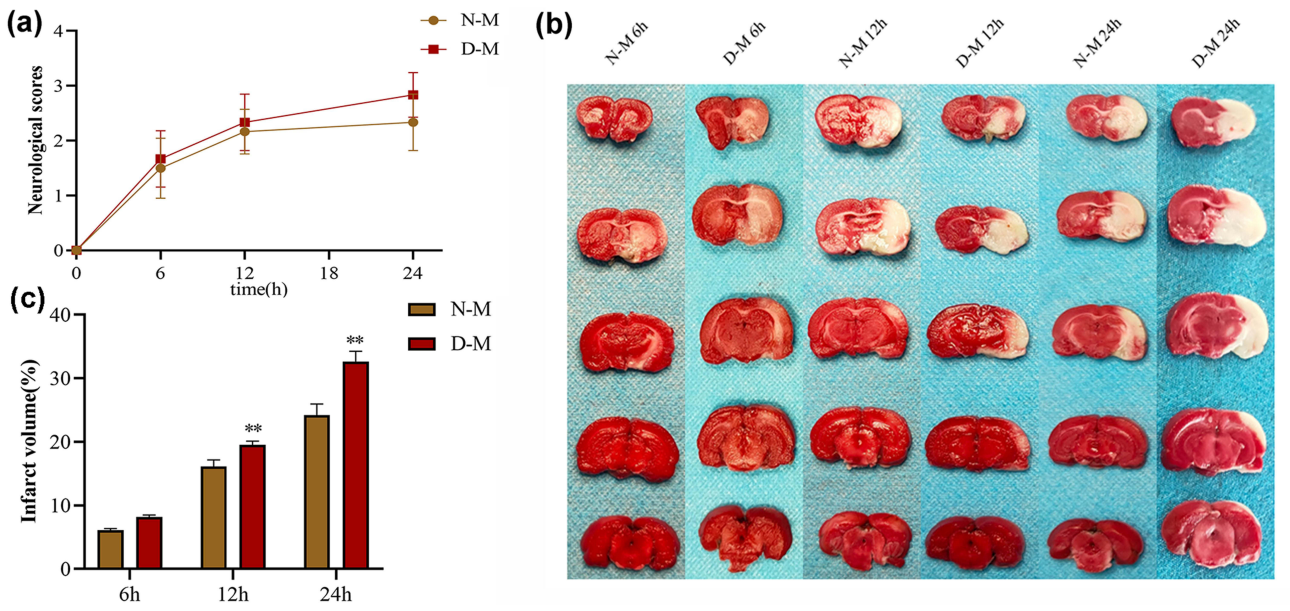

Figure 4 Effects of intestinal microbiota disorder on neurological function score and cerebral infarction volume at different time after cerebral ischemia.
Notes: (**a**) Neurological function score; (**b** and **c**) Cerebral infarction volume. n = 18. **P < 0.01 vs N-M.

Effects of Naotaifang III on LPS in Blood Plasma and Brain Cortex, and IL-1β in Brain Cortex

As shown in Figure 6, the levels of LPS in plasma, LPS, and IL-1β in brain cortex of the N-M group were increased to different degrees compared to those of the N-S group. Compared with the N-M group, the D-M group presented remarkable increasement of LPS and IL-1β (n = 6, P < 0.05). In the NTF and ZY groups, the levels of LPS and IL-1β were significantly decreased compared to those of the D-M group (n = 6, P < 0.01, P < 0.05). These data suggested that Naotaifang III may exert anti-inflammation to ameliorate cerebral ischemia injury.

Effects of Naotaifang III on TLR4 and NF-κB Expression in Brain Cortex

As shown in Figures 7 and 8, immunofluorescence staining and Western blot were used to observe the expression of TLR4 and NF-κB. The protein expressions of TLR4 and NF-κB in the N-M group were significantly higher than those in the N-S group (n = 3, P < 0.01, P < 0.05). Compared with the N-M group, the expressions of TLR4 and NF-κB in the D-M group were significantly increased (n = 3, P < 0.01, P < 0.05). However, in the NTF and ZY groups, the protein expressions of TLR4 and NF-κB were significantly lower than those in the D-M group, indicating that Naotaifang III treatment may inhibit neuroinflammation by inhibiting the LPS/TLR4/NF-κB signaling pathway.

Effects of Naotaifang III on Intestinal Microbiota Diversity

In order to explore the effects of Naotaifang III on the intestinal microbiota of ischemic stroke rats, we randomly selected five rats in N-M, D-M, and NTF to sequence 16S rDNA gene. VENN and Upset plot were used to analyse and compare the OTUs in each group to preliminarily understand the species composition characteristics of each group. As shown in Figure 9a, the total OUTs of N-M, D-M, and NTF groups were 655, 458, and 735, respectively, of which 387 OTUs were shared by the three groups. The number of OTUs shared by N-M and NTF groups was 591, which was significantly higher than the number of OTUs shared by N-M and D-M groups, as well as D-M and NTF groups.

Based on OTU, alpha diversity analysis was performed. The results showed that compared with the N-M group, the Sob, Chao1, and PD-tree index of the D-M group decreased significantly, but compared with the D-M group, the Sob, Chao1, and PD-tree index of the NTF group increased significantly (Figure 9b). These results indicated that the species of intestinal microbiota and the evenness of species in the D-M group were significantly reduced after gastric transplantation, resulting in

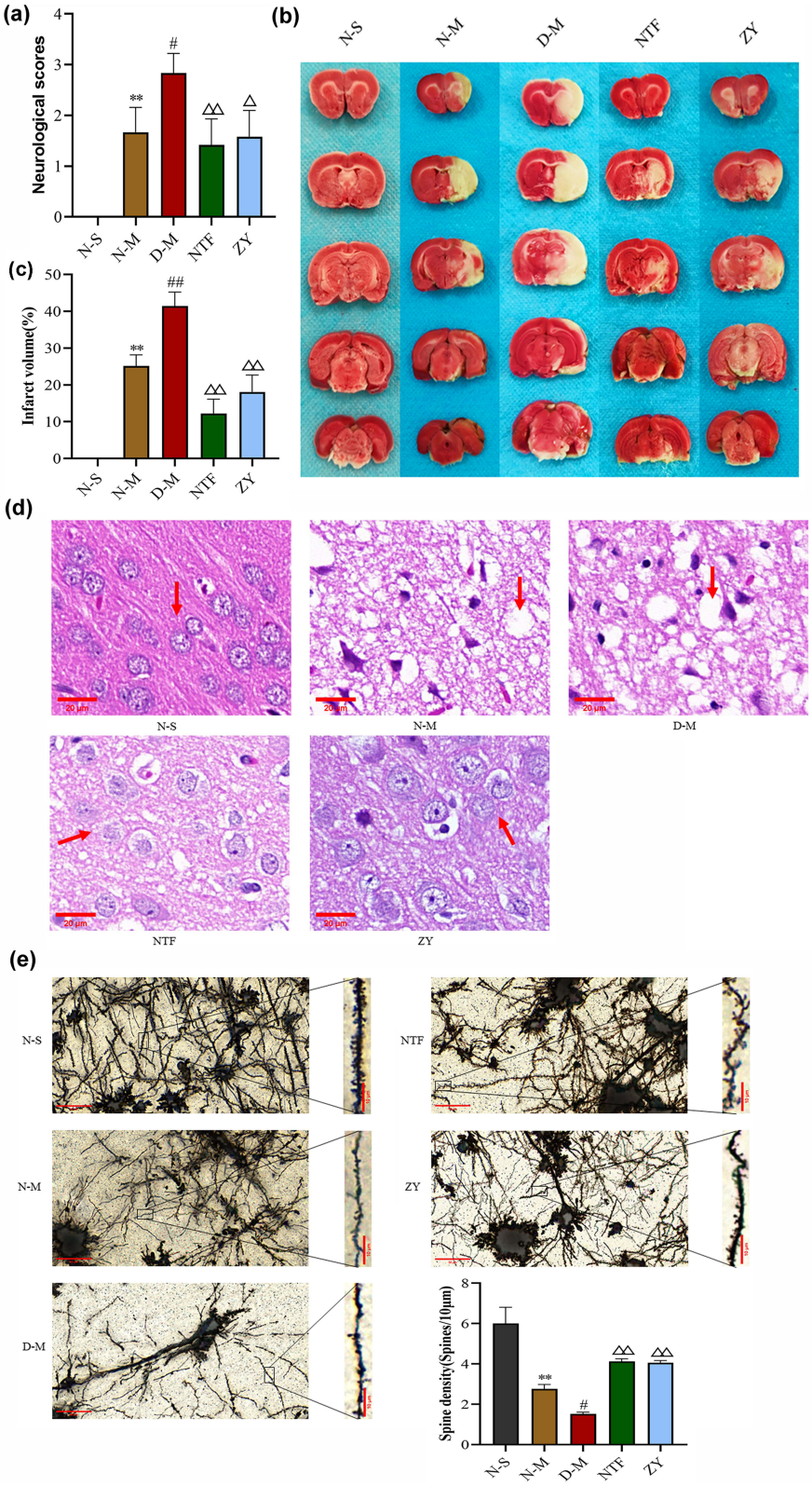

Figure 5 Effects of Naotaifang III on the cerebral injury.

Notes: (**a**) Neurological function score (n = 15); (**b** and **c**) Cerebral infarction volume (n = 3); (**d**) HE staining (×400, n = 3); (**e**) Golgi staining (× 400 and × 1000, n = 3). The values are the mean ± SEM. $^{**}P < 0.01$ vs N-S; $^{\#}P < 0.05$ vs N-M; $^{\#\#}P < 0.01$ vs N-M; $^{\Delta}P < 0.05$ vs D-M; $^{\Delta\Delta}P < 0.01$ vs D-M.

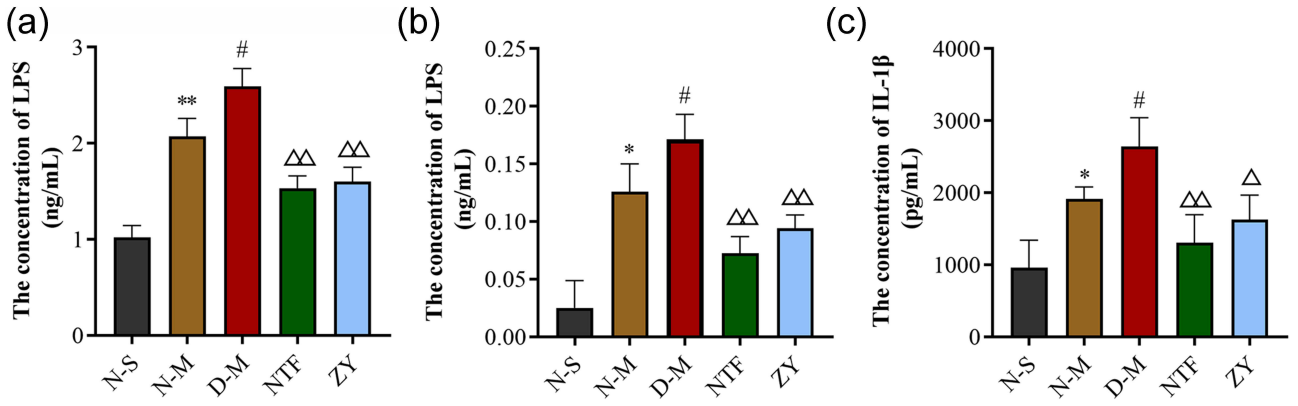

Figure 6 Effects of Naotaifang III on LPS in blood plasma and brain cortex, IL-1β in brain cortex.
Notes: (**a**) Levels of LPS in blood plasma; (**b**) Levels of LPS in brain cortex; (**c**) Levels of IL-1β in brain cortex. The values are the mean ± SEM. n = 6. *P < 0.05 vs N-S; **P < 0.01 vs N-S; #P < 0.05 vs N-M; ΔP < 0.05 vs D-M; ΔΔP < 0.01 vs D-M.

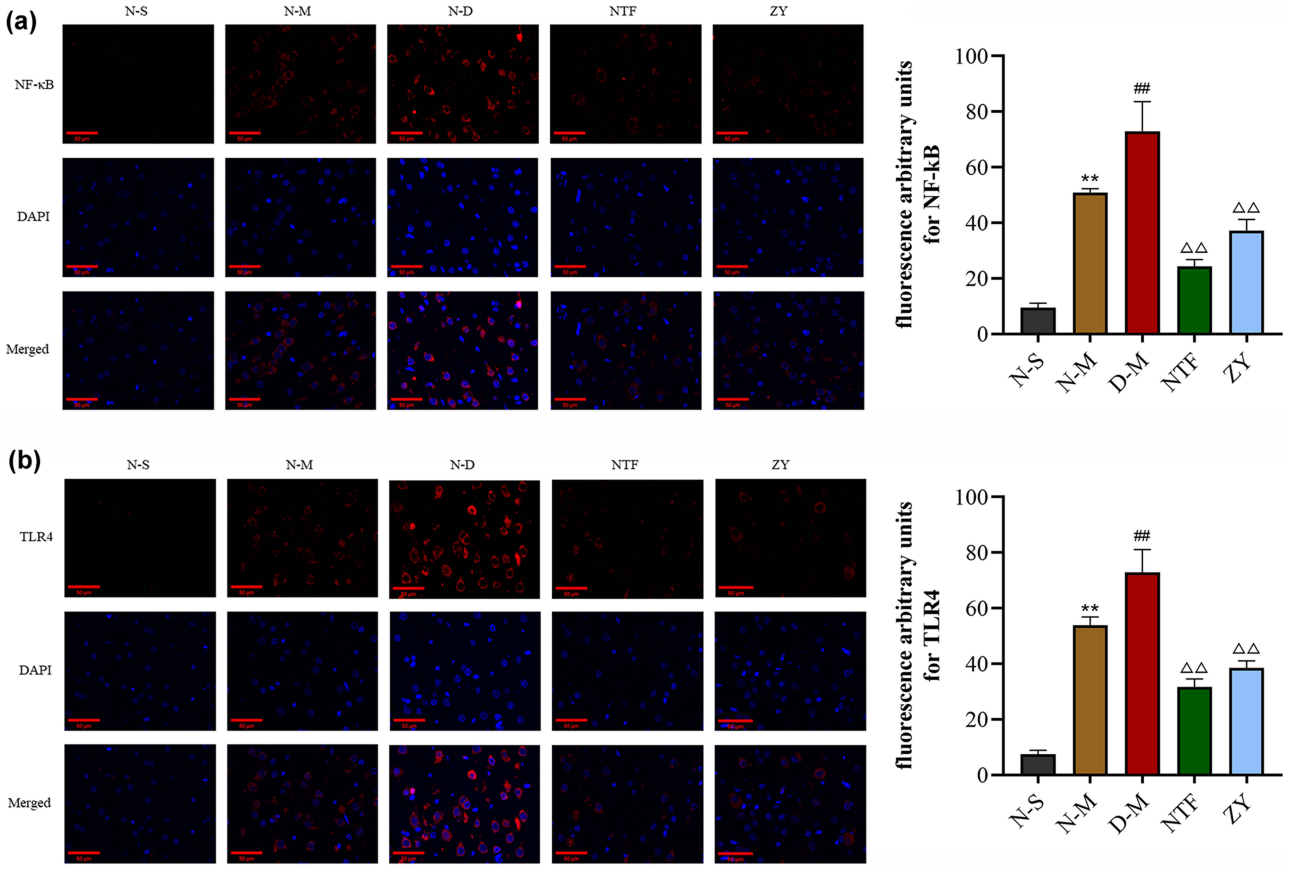

Figure 7 Effects of Naotaifang III on TLR4 and NF-κB expression in brain cortex (immunofluorescence staining, 400×).
Notes: (**a**) Immunofluorescence staining of TLR4; (**b**) Immunofluorescence staining of NF-κB; The values are the mean ± SEM. n = 3. **P < 0.01 vs N-S; ##P < 0.01 vs N-M; ΔΔP < 0.01 vs D-M.

a significant decrease in alpha diversity of the D-M group, while the alpha diversity in the NTF group was significantly increased. In addition, the sparse curves corresponding to the three parameters showed that with the deepening of sequencing, the curves of each sample tended to be flat (Figure 9c), indicating that the sequencing depth had covered all species in the sample, further increasing the sequencing depth. This showed that the changes in α-diversity in the D-M and NTF groups were caused by microbiota transplantation and Naotaifang III, respectively, rather than by the sequencing process.

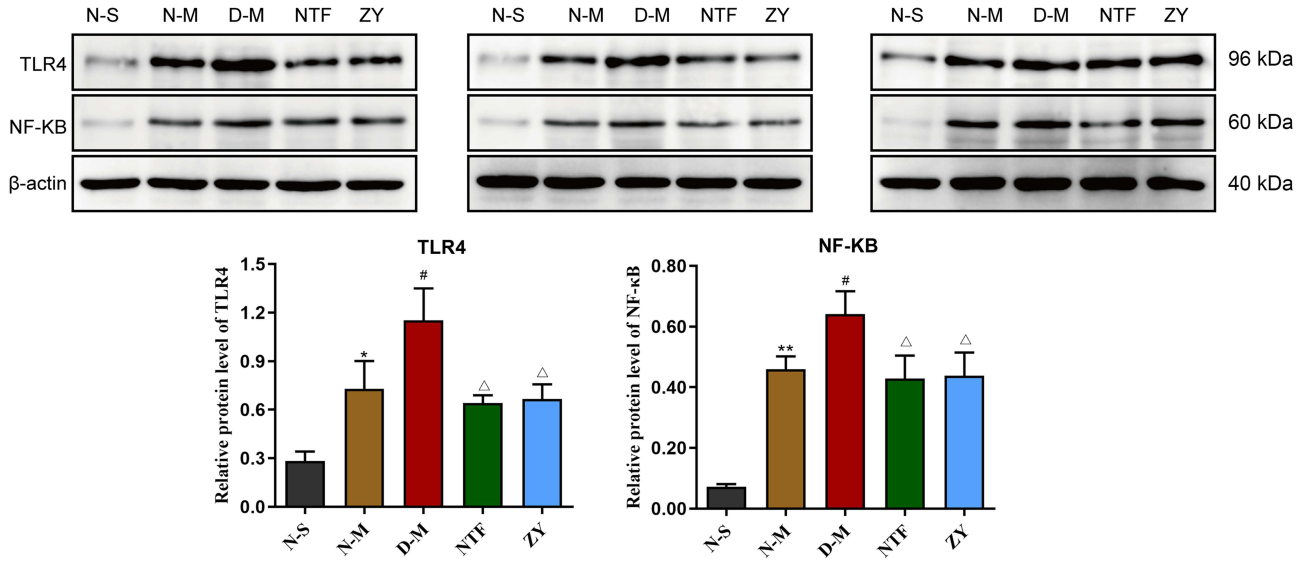

Figure 8 Effects of Naotaifang III on TLR4 and NF-κB expression in brain cortex (Western blot).
Notes: The values are the mean ± SEM. n = 3. *P < 0.05 vs N-S; #P < 0.05 vs N-M; ##P < 0.01 vs N-M; △P < 0.05 vs D-M.

Furthermore, to understand the effect of Naotaifang III on the distribution of gut microbiota, principal coordinate analysis (PCoA), non-metric multidimensional scaling (NMDS), and heatmap of BrayCurtis distance were performed based on OTU (Figure 9d). The results showed that the PCoA and NMDS scatter plots of the D-M group and the NTF group were significantly separated. However, the PCoA and NMDS scatter plots of the N-M group and the NTF group were relatively close. Interestingly, the heatmap of BrayCurtis distance also showed similar trends to PCoA and NMDS. These results indicated that the composition of gut microbiota was significantly changed after microbiota transplantation, and Naotaifang III treatment could significantly suppress the abnormal changes, making it closer to the N-M group.

Effects of Naotaifang III on Intestinal Microbiota Structure

In order to further understand the abnormal changes of intestinal microbiota in ischemic stroke rats and the effect of Naotaifang III on it, we analyzed the differences between groups at the phylum, class, and genus levels. At the phylum level (Figure 10a), the relative abundance of Firmicutes was significantly decreased in the D-M group compared with the N-M group, but significantly increased after Naotaifang III treatment. However, compared with the N-M group, the relative abundance of Bacteroides in the D-M group was significantly increased, while it was significantly decreased after Naotaifang III treatment. At the category level (Figure 10b), we can see that the abundance of Bacteroides in the D-M group is higher than that in the N-M and NTF groups, but the abundance of Clostridium is lower than that in the N-M and NTF groups. The ternary phase diagram of species at the genus level showed that the abundances of prevotella_9 and Bacteroidetes were significantly lower in the NTF group than in the N-M and D-M groups (Figure 10c). These results indicated that the gut microbiota structure changed significantly after gastric transplantation, manifested as an increase in Gram-negative bacteria and a decrease in Gram-positive bacteria, which could be reversed by Naotaifang III. In summary, our findings suggest that Naotaifang III can effectively alleviate the abnormal changes in gut microbiota structure.

Effects of Naotaifang III on Intestinal Microbiota Function

We used PICRUSt to predict gut microbiota function in each group of rats. The results showed that the N-M group and the D-M group had almost the same function of gut microbiota, but there were significant differences in the synthesis and degradation of ketone bodies. However, compared with the D-M group, the intestinal microbiota function in the NTF group changed significantly, mainly including antibiotic biosynthesis, citric acid cycle, lipopolysaccharide biosynthesis,

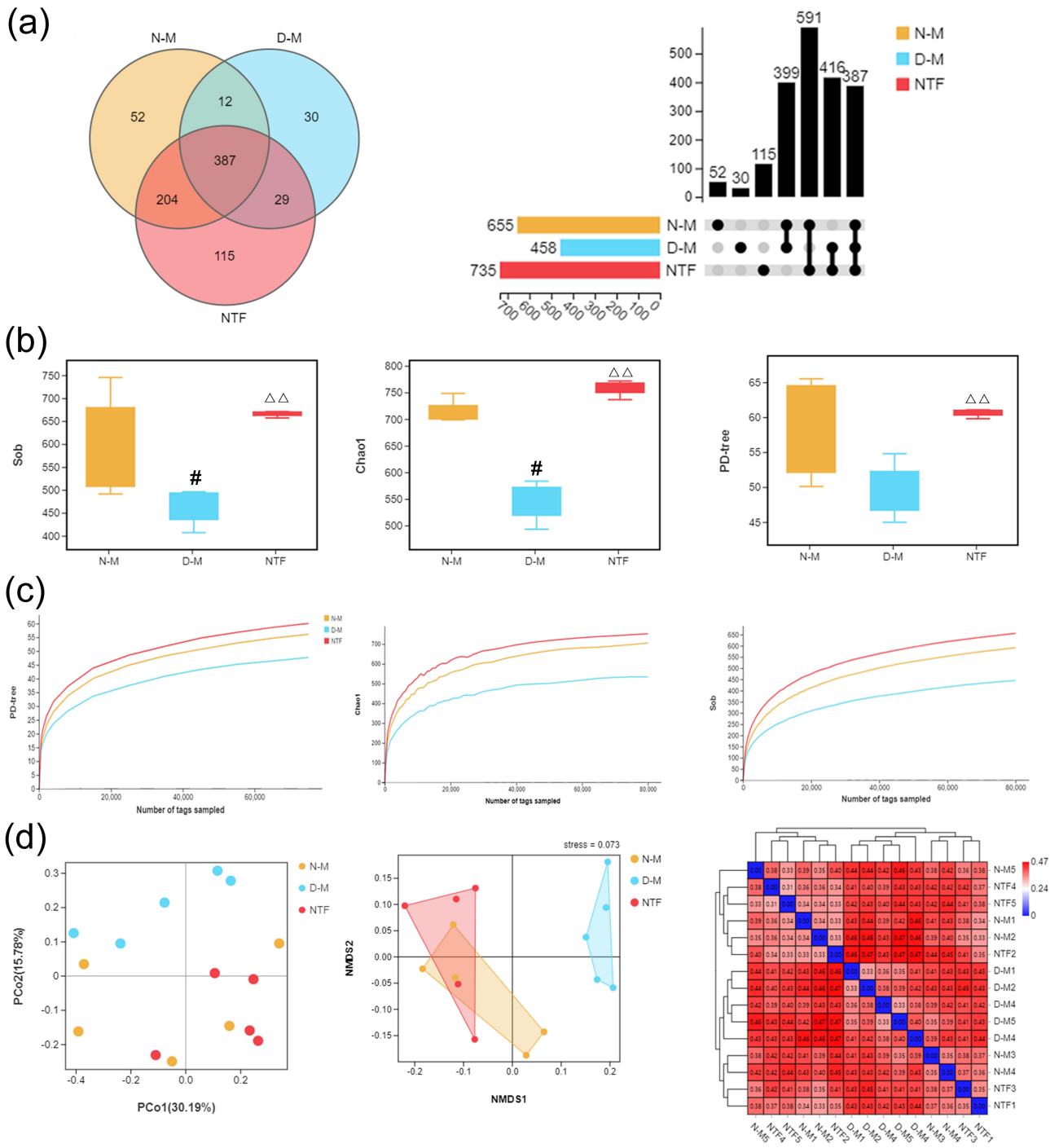

Figure 9 Effects of Naotaifang III on intestinal microbiota diversity.
Notes: (**a**) VENN and Upset plot of OTU levels; (**b**) Intestinal microbiota alpha diversity parameters. (**c**) Rarefaction curves. (**d**) PCoA, NMDS, and distance thermal graph. Data are expressed as the mean ± SD, n = 5. $^{\#}P < 0.05$ vs N-M; $^{\Delta\Delta}P < 0.01$ vs D-M.

panquinone and other terpenoid-quinone biosynthesis, oxidative phosphorylation, glutathione metabolism, toluene degradation, fatty acid degradation, phenylalanine metabolism, tyrosine metabolism, peroxisome, phosphoinositol metabolism, and iron-carrier-based non-ribosomal peptide biosynthesis in the vancomycin group ($P < 0.05$ or 0.01) (Figure 11). These results suggest that Naotaifang III can effectively alleviate intestinal microbiota dysfunction.

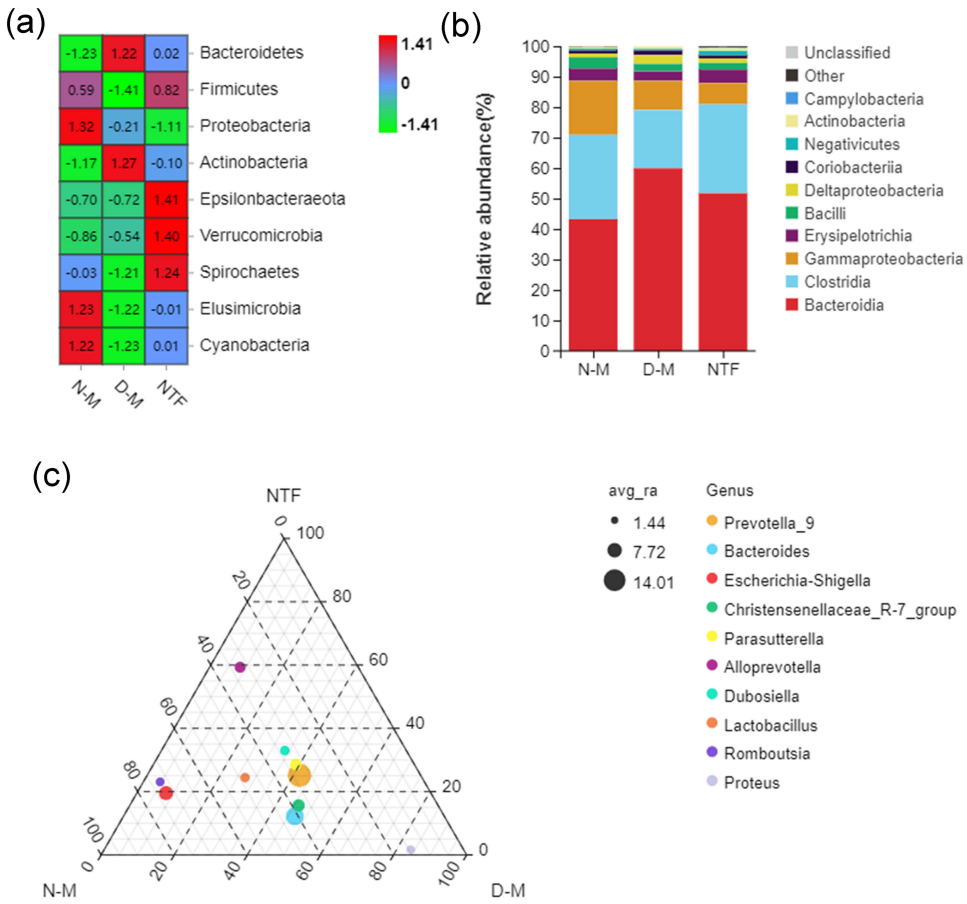

Figure 10 Effects of Naotaifang III on intestinal microbiota structure.
Notes: (**a**) Heat map of species composition at phylum level; (**b**) Stack map of species at class level. (**c**) Ternary phase diagram of species at genus level.

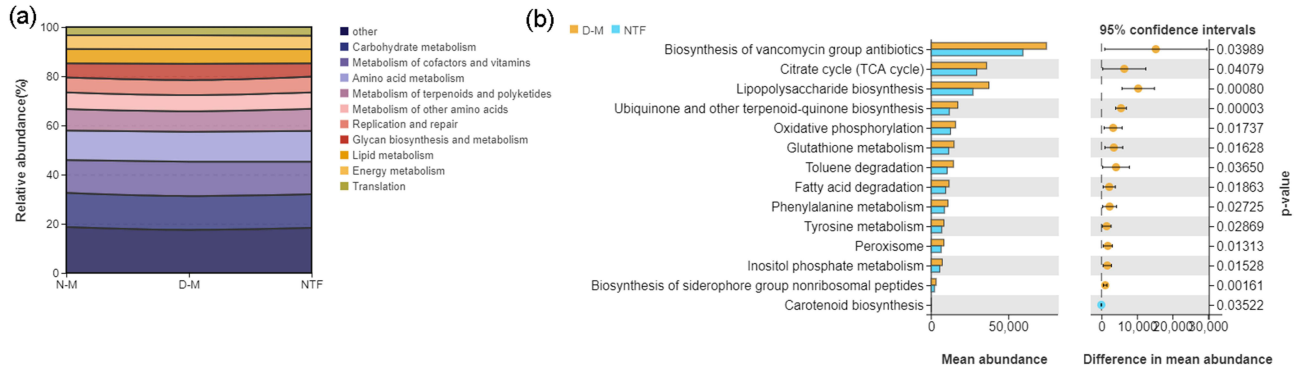

Figure 11 Effects of Naotaifang III on intestinal microbiota function.
Notes: (**a**) PICRUSt function prediction chart; (**b**) Differential functional test analysis.

Discussion

Ischemic stroke is characterized by high morbidity, mortality, and disability rates, placing a heavy economic burden on the patient's family and society. An increasing number of studies have indicated that the intestinal microbiome can affect the occurrence of IS by regulating risk factors of IS, such as hypertension and atherosclerosis,[22,23] and participate in the development and prognosis of IS through immune and metabolic systems and inflammatory pathways,[24,25] which were considered to be key participants in IS.[26] When choosing an animal model, considering that IS can lead to an imbalance of intestinal flora,[8,27,28] previous studies directly used animal models of cerebral ischemia to explore the effect of

intestinal microbiota dysbiosis on cerebral ischemia injury.[29–31] In order to better explain the relationship between gut microbiota imbalance and cerebral ischemia injury, we used a rat model of cerebral ischemia with a similar gut microbiota structure established in our previous study.[32] This model can create a state of intestinal dysbiosis similar to cerebral ischemia in rats. This approach to modeling gut microbiota imbalances is simple and reproducible (Figure 10).

Current studies have shown that cerebral ischemia can rapidly cause intestinal ischemia and produce excess nitrate through free radical reactions, resulting in intestinal flora imbalance and an increase in Enterobacteriaceae.[33] Enterobacteriaceae enrichment exacerbates cerebral infarction by enhancing systemic inflammation and is an independent risk factor for major adverse outcomes in stroke patients.[26] Dramatic changes in the gut microbiome and its metabolites lead to inflammation and oxidative stress in the gut. For example, the excessive proliferation of Enterobacteriaceae aggravates the occurrence of systemic inflammation and worsens cerebral infarction through the LPS-TLR4 pathway.[33] As an important member of TLRs, TLR4 plays an important role in the induction and regulation of immune inflammatory response.[34] In the central nervous system, TLR4 is mainly expressed in microglia and astrocytes in the central nervous system, and is an important regulator of neuroimmune inflammatory responses.[35] Studies have shown that during IS, the immune response to the ischemic process mainly mobilizes circulating cells, which, upon activation, will be recruited to the site of injury.[36] At the same time, intracellular molecules are released into the extracellular space through uncontrolled cell death. These molecules can bind to TLR4 in circulating immune cells (eg, monocytes, macrophages, neutrophils, etc.), which are then activated, triggering an inflammatory response.[37] TLRs play an important role in the induction and regulation of immune inflammatory responses, especially TLR4. TLR4 is mainly expressed in microglia and astrocytes in the central nervous system and is an important regulator of neuroinflammatory responses.[35] It was found that the expression of TLR4 was positively correlated with NF-κB, IL-1β, and cerebral infarct volume after 72 h of cerebral ischemia in rats.[38] The volume of cerebral infarction in TLR4 knockout mice was significantly reduced, and the TLR4 inhibitor TAK-242 could significantly reduce cerebral ischemic injury.[39] It has been reported that TLRs play a key role in the communication between the gut microbiota and the host,[40] and LPS of Gram-negative bacteria is a specific ligand for TLR4, which can stimulate the body's innate immune cells to produce an immune inflammatory response.[9] TLR4-mediated microglia/macrophage polarization and neutrophil dynamics may be involved in all aspects of neutrophil roles in stroke pathology, from activation to migration to execution of their functions in injured tissues.[41,42]

In this study, neurological scores and cerebral infarct volumes were compared between normal rats and rats with intestinal dysbiosis at 6h, 12h, and 24h after MCAO cerebral ischemia. We found that gut microbiota imbalance aggravated neurological impairment after IS, and the volume of cerebral infarction increased significantly, most notably at 24 h (Figure 4). Another study found that LPS in brain tissue increased significantly after 24 hours of cerebral ischemia.[43] In addition, the expression of TLR4 gradually increased after cerebral ischemia, reaching a peak at 24 hours.[44,45] Therefore, 24h was selected as the time point of IS for the follow-up study. This study found that Naotaifang III could improve the neurological damage of cerebral ischemia, reduce the volume of cerebral infarction, increase the density of dendritic spines of nerve cells, and improve the pathological morphological damage (Figure 5). In addition, we found that Naotaifang III reduced LPS levels in plasma, cerebral cortex, and IL-1β levels in cerebral cortex (Figures 6 and 7). It can also inhibit the expression of TLR4 and NF-κB proteins in the cerebral cortex. These results suggest that Naotaifang III may inhibit neuroinflammation by reducing LPS levels in peripheral blood and brain tissue, thereby inhibiting the expression of TRL4 and NF-κB proteins. In addition, the ZY group was set up for comparison. The results showed that LPS, TLR4, NF-κB, and IL-1β in the D-M group were significantly decreased after transplantation of normal bacteria. However, Naotaifang III showed a more significant decrease than the ZY group, which may be the reason why Naotaifang III acts not only on the gut but also on the blood and brain.

In order to uncover the mechanism of how Naotaifang affects gut microbes, we utilized 16S rDNA sequencing analysis and found that Naotaifang III could increase the diversity of intestinal microbiota in rats with cerebral ischemia, improve the structure of the flora, and regulate the function of the intestinal microbiota (Figures 8–10). Through the analysis of bacterial flora diversity, we found that the abundance and richness of the flora in the Naotaifang III group were higher than those in the N-M group, suggesting that the intestinal microbiota may have been unbalanced after 24 hours of cerebral ischemia in normal rats. From the analysis of the flora structure, we found that Firmicutes increased significantly and Bacteroidetes decreased significantly in Naotaifang III group. Firmicutes and Bacteroidetes are the

dominant flora in the intestinal microbiota, accounting for about 95% of the intestinal microbiota.[46] Bacteroidetes are Gram-negative bacteria, and Firmicutes are Gram-positive bacteria. These results suggest that Naotaifang III can reduce the number of Gram-negative bacteria in the intestinal microbiota, thereby reducing the production of LPS. Current studies have shown that LPS of Gram-negative bacteria is a specific ligand for TLR4, which can stimulate the body's innate immune cells to produce immune inflammatory responses.[43,47,48] Further analysis of the function of the flora showed that Naotaifang III could reduce the biosynthesis of vancomycin antibiotics, citric acid cycle, lipopolysaccharide biosynthesis, panquinone biosynthesis, oxidative phosphorylation, glutathione metabolism, toluene degradation, fatty acid degradation, phenylalanine metabolism, and tyrosine metabolism. These results further suggest that Naotaifang III can inhibit the biosynthesis of LPS.

The limitation of this study is that although we performed quality control by HPLC, we did not study the main active components of Naotaifang III, which will affect the precise exploration of the mechanism of the brain-gut axis after Naotaifang III intervention in IS. In the future, we will further explore the role of core components of Naotaifang III (such as astragaloside IV, ligustrazine, rhein, and other components) in the brain-gut axis of cerebral ischemia to further explore its mechanism.

Conclusion

Based on the present results, Naotaifang III may play a protective role in IS by inhibiting neuroinflammatory damage through the LPS/TLR4 signaling pathway in the microbe-gut-brain axis. However, the metabolomic analysis of Naotaifang III in blood and brain remains to be further investigated.

Data Sharing Statement

The data underlying this article will be shared upon reasonable request to the corresponding author.

Informed Consent Statement

All animal care and protocols were performed in accordance with the Guidelines for Animal Experimentation and were approved by the Animal Ethics Committee of Hunan University of Chinese Medicine.

Author Contributions

All authors made a significant contribution to the work reported, whether that is in the conception, study design, execution, acquisition of data, analysis and interpretation, or in all these areas; took part in drafting, revising, or critically reviewing the article; gave final approval of the version to be published; have agreed on the journal to which the article has been submitted; and agree to be accountable for all aspects of the work.

Funding

This work was supported by Natural Science Foundation of Hunan Province (No. 2022JJ40303) and Scientific Research Fund of Hunan University of Chinese Medicine (No. 2021XJJJ022).

Disclosure

The authors declare no conflicts of interest regarding the publication of this article.

References

1. Virani SS, Alonso A, Benjamin EJ, et al.; American Heart Association Council on Epidemiology and Prevention Statistics Committee and Stroke Statistics Subcommittee. Heart disease and stroke statistics-2020 update: a report from the American Heart Association. *Circulation*. 2020;141(9):139–596.
2. Rabinstein AA. Update on treatment of acute ischemic stroke. *Continuum*. 2020;26(2):268–286. doi:10.1212/CON.0000000000000840
3. Zhou Y, Yan S, Song X, et al. Intravenous thrombolytic therapy for acute ischemic stroke in Hubei, China: a survey of thrombolysis rate and barriers. *BMC Neurol*. 2019;19(1):202. doi:10.1186/s12883-019-1418-z
4. Lahr MM, Luijckx GJ, Vroomen PC, van der Zee DJ, Buskens E. Proportion of patients treated with thrombolysis in a centralized versus a decentralized acute stroke care setting. *Stroke*. 2012;43(5):1336–1340. doi:10.1161/STROKEAHA.111.641795
5. Battaglini D, Pimentel-Coelho PM, Robba C, et al. Gut microbiota in acute ischemic stroke: from pathophysiology to therapeutic implications. *Front Neurol*. 2020;25:598. doi:10.3389/fneur.2020.00598

6. Spychala MS, Venna VR, Jandzinski M, et al. Age-related changes in the gut microbiota influence systemic inflammation and stroke outcome. *Ann Neurol*. 2018;84(1):23–36. doi:10.1002/ana.25250
7. Li N, Wang X, Sun C, et al. Change of intestinal microbiota in cerebral ischemic stroke patients. *BMC Microbiol*. 2019;19(1):191. doi:10.1186/s12866-019-1552-1
8. Singh V, Sadler R, Heindl S, et al. The gut microbiome primes a cerebroprotective immune response after stroke. *J Cereb Blood Flow Metab*. 2018;38(8):1293–1298. doi:10.1177/0271678X18780130
9. Opazo MC, Ortega-Rocha EM, Coronado-Arrázola I, et al. Riedel intestinal microbiota influences non-intestinal related autoimmune diseases. *Front Microbiol*. 2018;9:432. doi:10.3389/fmicb.2018.00432
10. Chen R, Wu P, Cai Z, et al. Puerariae Lobatae Radix with chuanxiong Rhizoma for treatment of cerebral ischemic stroke by remodeling gut microbiota to regulate the brain-gut barriers. *J Nutr Biochem*. 2019;65:101–114. doi:10.1016/j.jnutbio.2018.12.004
11. Yang XW, Li YH, Zhang H, et al. Safflower Yellow regulates microglial polarization and inhibits inflammatory response in LPS-stimulated Bv2 cells. *Int J Immunopathol Pharmacol*. 2016;29(1):54–64. doi:10.1177/0394632015617065
12. Lan B, Ge JW, Cheng SW, et al. Extract of Naotaifang, a compound Chinese herbal medicine, protects neuron ferroptosis induced by acute cerebral ischemia in rats. *J Integr Med*. 2020;18(4):344–350. doi:10.1016/j.joim.2020.01.008
13. He YH, Hao XY, Ge JW. Clinical study of naotai formula in treating cerebral infarction with Qi deficiency and blood stasis syndrome. *J Emerg Trad Chin*. 2001;10(6):1–4.
14. Yi YQ, Liu J, Liu L, et al. Protective effects of Jiawei Naotai Formula on hippocampal neurons induced by hypoxia/reoxygenation based on SIRT1-mediated apoptosis-related signaling pathway. *Chin J Trad Chin Med Pharm*. 2019;34(10):4516–4522.
15. Yi YQ, Liu J, Liu L, et al. Effects of modified naotai prescription on inflammatory pathway of SIRT1/NF-κB in Hypoxia/Reoxygenation injured hippocampal neuron. *Chin J Inform Trad Chin Med*. 2019;26(03):45–50.
16. Liang JH, Zheng KW, Jing DW. Study on the regulatory effect of APS on intestinal flora in rats with ulcerative colitis. *Chin J Trad Med Sci Technol*. 2012;19(04):331–332.
17. Yu XH, Zhu YQ, Wang YJ, Xu YP, Guo Y. Effects of rhubarb anthraquinone glycoside on cerebral ischemia-reperfusion injury and intestinal flora in rats. *Chin Trad Patent Med*. 2019;41(05):1151–1155.
18. Wu WF, Nie HF, Hu LJ, et al. Effect of Buyang Huanwu Decoction on gut microbiota and plasma metabolites in ischemic stroke rats with qi deficiency and blood stasis syndrome. *Chin Trad Herbal Drugs*. 2021;52(01):118–128.
19. Wu WF, Cheng C, Nie HF, et al. Study on effects of gut microbiota of Qi deficiency and blood stasis syndrome ischemic stroke rats on the absorption of effective ingredients in Buyang Huanwu Decoction. *J Hunan Univ Chin Med*. 2020;40(06):666–672.
20. Yang T, Chen X, Mei Z. An integrated analysis of network pharmacology and experimental validation to reveal the mechanism of Chinese medicine formula naotaifang in treating cerebral ischemia-reperfusion injury. *Drug Des Devel Ther*. 2021;15:3783–3808. doi:10.2147/DDDT.S328837
21. Longa EZ, Weinstein PR, Carlson S, et al. Reversible middle cerebral artery occlusion without craniectomy in rats. *stroke*. 1989;20(1):84–91. doi:10.1161/01.STR.20.1.84
22. Yang T, Santisteban MM, Rodriguez V, et al. Mohamadzadeh Gut dysbiosis is linked to hypertension. *Hypertension*. 2015;65(6):1331–1340. doi:10.1161/HYPERTENSIONAHA.115.05315
23. Li J, Zhao F, Wang Y, et al. Gut microbiota dysbiosis contributes to the development of hypertension. *Microbiome*. 2017;5(1):14. doi:10.1186/s40168-016-0222-x
24. Lukiw WJ, Cong L, Jaber V, Zhao Y. Microbiome-Derived Lipopolysaccharide (LPS) Selectively Inhibits Neurofilament Light Chain (NF-L) Gene Expression in Human Neuronal-Glial (HNG) Cells in Primary Culture. *Front Neurosci*. 2018;12:896. doi:10.3389/fnins.2018.00896
25. Liu Q, Johnson EM, Lam RK, et al. Peripheral TREM1 responses to brain and intestinal immunogens amplify stroke severity. *Nat Immunol*. 2019;20(8):1023–1034. doi:10.1038/s41590-019-0421-2
26. Xu K, Gao X, Xia G, et al. Rapid gut dysbiosis induced by stroke exacerbates brain infarction in turn. *Gut*. 2021:gutjnl-2020–323263. PMID: 33558272. doi:10.1136/gutjnl-2020-323263
27. Nicholson SE, Watts LT, Burmeister DM, et al. Moderate traumatic brain injury alters the gastrointestinal microbiome in a time-dependent manner. *Shock*. 2019;52(2):240–248. doi:10.1097/SHK.0000000000001211
28. Durgan DJ, Lee J, McCullough LD, Bryan RM. Examining the role of the microbiota-gut-brain axis in stroke. *Stroke*. 2019;50(8):2270–2277. doi:10.1161/STROKEAHA.119.025140
29. Stanley D, Moore RJ, Wong CHY. An insight into intestinal mucosal microbiota disruption after stroke. *Sci Rep*. 2018;8(1):568. doi:10.1038/s41598-017-18904-8
30. Yu M, Zeng XZ. Research progress on the effect of intestinal flora on immune function after stroke. *J Apopl Nervous Dis*. 2020;37(10):943–945.
31. Zhang PP. Dysbiosis of gut microbiota can increase the risk of stroke, Hebei Medical University; 2018:4–18.
32. Nie H, Peng Z, You J, et al. Establishment of a microbial transplantation-induced dysbacteriosis model in rats with ischemic stroke. *Chin J Public Health*. 2022;38(03):314–319.
33. Deng F, Lin ZB, Sun QS, et al. The role of intestinal microbiota and its metabolites in intestinal and extraintestinal organ injury induced by intestinal ischemia reperfusion injury. *Int J Biol Sci*. 2022;18(10):3981–3992. PMID: 35844797; PMCID: PMC9274501. doi:10.7150/ijbs.71491
34. Andresen L, Theodorou K, Grünewald S, et al. Evaluation of the therapeutic potential of anti-TLR4-antibody MTS510 in experimental stroke and significance of different routes of application. *PLoS One*. 2016;11(2):e0148428. PMID: 26849209; PMCID: PMC4746129. doi:10.1371/journal.pone.0148428
35. Yao X, Liu S, Ding W, et al. TLR4 signal ablation attenuated neurological deficits by regulating microglial M1/M2 phenotype after traumatic brain injury in mice. *J Neuroimmunol*. 2017;310:38–45. doi:10.1016/j.jneuroim.2017.06.006
36. García-Culebras A, Durán-Laforet V, Peña-Martínez C, et al. Role of TLR4 (Toll-Like Receptor 4) in N1/N2 neutrophil programming after stroke. *Stroke*. 2019;50(10):2922–2932. PMID: 31451099.. doi:10.1161/STROKEAHA.119.025085
37. Durán-Laforet V, Peña-Martínez C, García-Culebras A, Alzamora L, Moro MA, Lizasoain I. Pathophysiological and pharmacological relevance of TLR4 in peripheral immune cells after stroke. *Pharmacol Ther*. 2021;228:107933. PMID: 34174279. doi:10.1016/j.pharmthera.2021.107933
38. Zhao Y, Wang H, Chen W, et al. Melatonin attenuates white matter damage after focal brain ischemia in rats by regulating the TLR4/NF-κB pathway. *Brain Res Bull*. 2019;150:168–178. doi:10.1016/j.brainresbull.2019.05.019

39. Hua F, Tang H, Wang J, et al. TAK-242, an antagonist for Toll-like receptor 4, protects against acute cerebral ischemia /reperfusion injury in mice. *J Cereb Blood Flow Metab*. 2015;35(4):536–542. doi:10.1038/jcbfm.2014.240
40. McKernan DP, Dennison U, Gaszner G, Cryan JF, Dinan TG. Enhanced peripheral toll-like receptor responses in psychosis: further evidence of a pro-inflammatory phenotype. *Transl Psychiatry*. 2011;1(8):36. doi:10.1038/tp.2011.37
41. Li R, Zhou Y, Zhang S, Li J, Zheng Y, Fan X. The natural (poly)phenols as modulators of microglia polarization via TLR4/NF-κB pathway exert anti-inflammatory activity in ischemic stroke. *Eur J Pharmacol*. 2022;914:174660. PMID: 34863710. doi:10.1016/j.ejphar.2021.174660
42. Durán-Laforet V, Peña-Martínez C, García-Culebras A, et al. Role of TLR4 in neutrophil dynamics and functions: contribution to stroke pathophysiology. *Front Immunol*. 2021;12:757872. PMID: 34745132; PMCID: PMC8566541. doi:10.3389/fimmu.2021.757872
43. Kurita N, Yamashiro K, Kuroki T, et al. Metabolic endotoxemia promotes neuroinflammation after focal cerebral ischemia. *J Cereb Blood Flow Metab*. 2020;40(12):2505–2520. doi:10.1177/0271678X19899577
44. Qiao H, Zhang X, Zhu C, et al. Luteolin downregulates TLR4, TLR5, NF-κB and p-p38MAPK expression, upregulates the p-ERK expression, and protects rat brains against focal ischemia. *Brain Res*. 2012;1448:71–81. doi:10.1016/j.brainres.2012.02.003
45. Zheng SM, Li SY, Niu XL, Yang YM, Xue RL. Protective effect and mechanism of polymyxin B on the damage induced by lipopolysaccharide in rats during global cerebral ischemia-reperfusion. *J Guizhou Med Univ*. 2021;46(09):1011–1017.
46. Yamashita T, Emoto T, Sasaki N, Hirata K . Gut Microbiota and Coronary Artery Disease. *Int Heart J*. 2016;57(06):663–671 doi:10.1536/ihj.16-414.
47. Hu J, Wang W, Hao Q, et al. Suppressors of cytokine signalling (SOCS)-1 inhibits neuroinflammation by regulating ROS and TLR4 in BV2 cells. *Inflamm Res*. 2020;69(1):27–39. PMID: 31707448. doi:10.1007/s00011-019-01289-x
48. Vartanian KB, Stevens SL, Marsh BJ, Williams-Karnesky R, Lessov NS, Stenzel-Poore MP. LPS preconditioning redirects TLR signaling following stroke: TRIF-IRF3 plays a seminal role in mediating tolerance to ischemic injury. *J Neuroinflammation*. 2011;8(1):140. PMID: 21999375; PMCID: PMC3217906. doi:10.1186/1742-2094-8-140